

# Influence of soot aerosol properties on the counting efficiency of PN-PTI instruments

Tobias Hammer<sup>1</sup>, Diana Roos<sup>1</sup>, Barouch Giechaskiel<sup>2</sup>, Anastasios Melas<sup>2</sup>, Konstantina Vasilatou<sup>1</sup>

<sup>1</sup>Department of Chemistry, Federal Institute of Metrology METAS, Bern-Wabern, 3003, Switzerland

<sup>2</sup> European Commission, Joint Research Centre (JRC), 21027 Ispra, Italy

*Correspondence to:* Konstantina Vasilatou (konstantina.vasilatou@metas.ch)

**Abstract.** In this work, we investigated the influence of different types of soot aerosol on the counting efficiency (CE) of instruments employed for the periodic technical inspection (PTI) of diesel vehicles. Such instruments report particle number (PN) concentration. Combustion aerosols were generated by a prototype bigCAST, a miniCAST 5201 BC, a miniCAST 6204 C and a miniature inverted soot generator (MISG). For comparison purposes, diesel soot was generated by a Euro 5b diesel test vehicle with by-passed diesel particulate filter (DPF). The size-dependent counting efficiency profile of six PN-PTI instruments was determined with each one of the aforementioned test aerosols. The results showed that the type of soot aerosol affected the response of the PN-PTI sensors in an individualised manner. Consequently, it was difficult to identify trends and draw conclusive results about which laboratory-generated soot is the best proxy for diesel soot. Deviations in the counting efficiency remained typically within 0.25 units when using laboratory-generated soot compared to Euro 5b diesel soot of similar mobility diameter (~50-60 nm). Soot with a mobility diameter of ~100 nm generated by the MISG, the lowest size we could achieve, resulted [in most cases](#) in similar counting efficiencies as that generated by the different CAST generators [at the same particle size](#) ~~for most of the PN-PTI instruments~~, showing that MISG may be a satisfactory - and affordable - option for PN-PTI verification.

## 1 Introduction

Soot particles emitted by transport sources can have adverse health effects (Kheirbek et al., 2016; US-EPA, 2019; WHO, 2021). To reduce particulate emissions, new procedures for the periodic technical inspection (PTI) of diesel vehicles based on the measurement of particle number (PN) concentration have recently been established in Switzerland, Germany, the Netherlands and Belgium, while other countries might follow in due time (EU, 2023; Vasilatou et al., 2022). Portable instruments known as PN-PTI counters are used for measuring particle number concentration (PNC) directly in the tailpipe of diesel vehicles equipped with a diesel particle filter (DPF) (Kesselmeier and Staudt, 1999; Melas et al., 2021, 2022, 2023). When the DPF is intact, the emitted PNC is low (typically up to a few thousand particles per cm<sup>3</sup>), whereas if the DPF is defect or tampered, PNC increases to several hundred thousand particles per cm<sup>3</sup> (Botero et al., 2023; Burtscher et al., 2019; Giechaskiel et al., 2022). In terms of particle mass concentration, a functioning DPF can reduce particulate emissions by up to a factor of 150 (Ligterink, 2018) while in terms of particle number concentration a solid particle number trapping efficiency of higher than 99 % has been reported in the literature (Frank, Adam et al., 2020). It has been shown that a small fraction (about 10 %) of vehicles with defective DPF is responsible for up to 80-90 % of the total fleet emissions (Burtscher et al., 2019; Kurniawan and Schmidt-Ott, 2006). The goal of PN-PTI procedures is to identify diesel

37 vehicles with compromised DPFs, thus ensuring that vehicles in operation maintain their performance as  
38 guaranteed by type-approval, without excessive degradation, throughout their lifetime (EU, 2023).

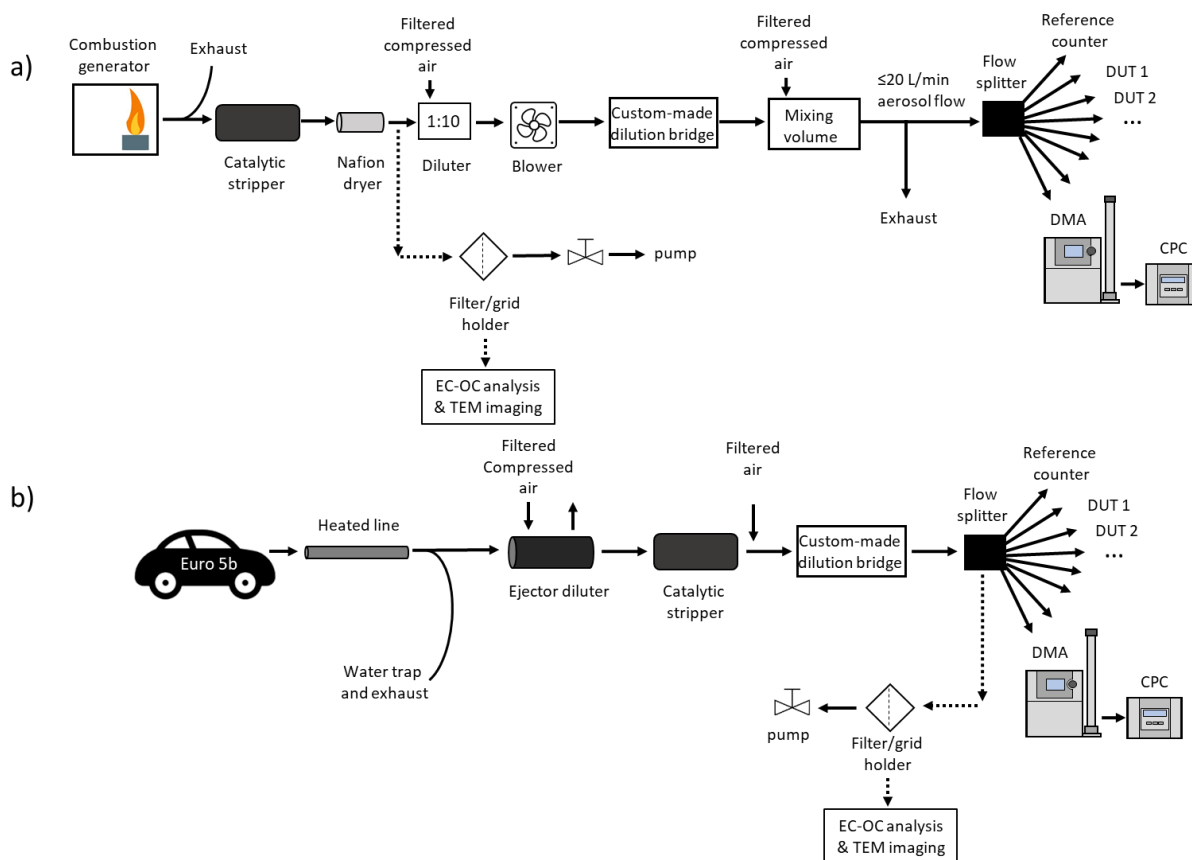
39 Although the concept of PN-PTI is simple, its implementation in practice is not as straightforward. PTI procedures  
40 are not fully harmonised and, as a result, the limit values for the emitted PNC, the technical specifications of the  
41 PN-PTI counters and the test protocol for type-examination and verification are defined at a national level (Anon,  
42 2019; AU-Richtlinie, n.d.; PTB, 2021; UVEK, 2023; VAMV, 2018; Vasilatou et al., 2022, 2023). Differences in  
43 national legislations might lead to contradicting results, e.g. the same diesel vehicle might pass the PTI check in  
44 one country but fail in another one. To ensure fair implementation of regulations across Europe and avoid  
45 unnecessary costs which may occur for vehicle owners after a False Fail, the various PTI procedures must be  
46 compared and the differences elucidated.

47 [PN-PTI instruments go through a type-examination procedure which may differ in each country. Among several](#)  
48 [tests, type-examination includes a counting efficiency and a linearity check typically performed with combustion](#)  
49 [aerosols. During their lifetime, PN-PTI instruments are checked for their linearity with polydisperse particles](#)  
50 [\(typically with a GMD of  \$70 \pm 20\$  nm\).](#) In our previous study (Vasilatou et al., 2023), we showed that the choice  
51 of test aerosol during type-examination or verification of PN-PTI instruments significantly affects the performance  
52 of instruments based on diffusion charging (DC). When sodium chloride (NaCl) or carbonaceous particles from  
53 spark-discharge generators were used as test aerosols, the counting efficiency of the DC-based instruments  
54 changed by up to a factor of two compared to that exhibited with diesel soot. The experiments clearly showed that  
55 soot from laboratory-based combustion generators was the best proxy for soot emitted by diesel engines, however,  
56 potential differences between the different combustion generators available on the market were not investigated.  
57 In this study, we challenged six different DC-based PN-PTI instruments with [polydisperse](#) soot particles produced  
58 by three different CAST generators (Jing AG, Switzerland), the miniature inverted soot generator (MISG,  
59 Argonaut Scientific, Canada) and a Euro 5b diesel vehicle. [The geometric mean diameter of the test aerosol was](#)  
60 [in the range used for linearity checks of PN-PTI instruments as well as in typical size range emitted by diesel](#)  
61 [engines. The scope of our study was to investigate possible differences that may arise when using different](#)  
62 [combustion aerosol generators during the type-examination and verification of PN-PTI instruments as well as to](#)  
63 [correlate with diesel engine emitted soot. We focused on DC-based instruments because we expect a larger impact](#)  
64 [of the aerosol properties on their response compared to CPC-based ones](#) (Vasilatou et al., 2023). The size-  
65 dependent counting efficiency of the PN-PTI instruments was determined by using a condensation particle counter  
66 (NPET 3795, TSI Inc., USA) as a reference instrument. We discuss the results in the context of the different  
67 national legislations and make recommendations for the harmonisation of the various calibration and verification  
68 procedures in the laboratory.

## 69 **2 Materials and methods**

70 During the first measurement campaign at METAS, the following laboratory-based [diffusion or premixed flame](#)  
71 generators were used to produce test aerosols: a prototype bigCAST, a miniCAST 5201 BC (Ess et al., 2021b; Ess  
72 and Vasilatou, 2019), a miniCAST 6204 C and the miniature inverted soot generator (MISG) (Giechaskiel and  
73 Melas, 2022; Kazemimanesh et al., 2019; Moallemi et al., 2019; Senaratne et al., 2023). By varying the operation  
74 points of the CAST generators, polydisperse aerosols with a geometric mean mobility diameter ( $GMD_{mob}$ ) ranging  
75 from 50 nm to 100 nm were generated, as summarised in Fig. S1. In the case of the MISG, particles with a  $GMD_{mob}$

76 down to 100 nm were produced in a repeatable and stable manner using a mixture of dimethyl ether and propane  
 77 (Senaratne et al., 2023). [This is in agreement with another study, where the modal diameter varied between 95 and](#)  
 78 [158 nm \(Bischof et al., 2020\).](#)  
 79 The counting efficiency profiles (CE) of six DC-based PN-PTI counters, namely the AEM (TEN, the Netherlands),  
 80 HEPaC (developed by the University of Applied Sciences Northwestern Switzerland and distributed by Naneos  
 81 GmbH, Switzerland), DiTEST (AVL DiTEST, Austria), CAP3070 (Capelec, France), DX280 (Continental  
 82 Aftermarket & Services GmbH, Germany) and AIP PDC KG4 (referred to as Knestel hereafter, KNESTEL  
 83 Technologie & Elektronik GmbH, Germany). The HEPaC, DiTEST, CAP3070 and DX280 had been type-  
 84 approved at METAS according to the Swiss regulations (VAMV, 2018) whereas the Knestel instrument had been  
 85 type-approved according to the German regulation (AU-Richtlinie, n.d.). The experimental setup at METAS is  
 86 depicted in Fig. 1a. Soot produced by CAST-burners or the MISG was passed through a catalytic stripper (Catalytic  
 87 Instruments GmbH, Germany), a Nafion dryer (MD-700-12S-1, PERMA PURE, U.S.A.), a VKL 10 diluter (Palas  
 88 GmbH, Germany) and a custom-made dilution bridge, and was mixed in a 27-ml-volume chamber. The aerosol  
 89 was split with a custom-made 8-port flow splitter and delivered simultaneously to the devices under test (DUT, in  
 90 this case PN-PTI instrument) and the reference particle counter (NPET 3795, TSI Inc., USA). [The NPET was](#)  
 91 [selected as reference instrument for two reasons: i\) it could be used in field measurements as it included a dilution](#)  
 92 [system, a volatile particle remover and a particle counter. ii\) during type examination portable PN-PTI instruments](#)  
 93 [are typically used as reference.](#) NPET had been calibrated in a traceable manner according to the ISO 27891  
 94 standard, and showed a CE of  $0.77 \pm 0.02$ ,  $0.77 \pm 0.01$ ,  $0.80 \pm 0.01$  and  $0.79 \pm 0.02$  at a  $GMD_{mob}$  of 50 nm, 70 nm,  
 95 80 nm and 100 nm, respectively [and this counting efficiency was taken into account during data analysis.](#)



96  
 97 **Figure 1: a) Experimental setup for the verification of PN-PTI instruments in the laboratory. Four different combustion**  
 98 **generators were used (see text for more details). DUT stands for device under tested. Dashed arrows designate**

99 **measurements which were performed separately, i.e. not in parallel with PN-PTI verification. b) Experimental setup as**  
100 **used for field measurements at JRC.**

101 Mobility size distributions were recorded simultaneously by a scanning mobility particle sizer (<sup>85</sup>Kr source 3077A,  
102 DMA 3081 and butanol CPC 3776, TSI Inc., USA). To analyse the morphology of the soot particles, particles  
103 were sampled for 5 s with a flow rate of 1.2 L/min downstream the Nafion dryer, collected on copper-coated TEM  
104 (transmission electron microscopy) grids placed in a mini particle sampler (MPS, Ecomeasure, France) and  
105 analysed with a Spirit Transmission EM (Tecnai, FEI Company, USA). Soot particles were also sampled on QR-  
106 100 Advantec filters (Toyo Roshi Kaisha, Ltd. Japan, preheated at 500 °C for > 1 h) for durations of 15 – 30 min.  
107 Elemental carbon (EC) to total carbon (TC) mass fractions were measured with an OC/EC Model 5L analyser  
108 (Sunset Laboratory Inc., NL) by applying an extended EUSAAR-2 protocol (Ess et al., 2021b, 2021a).

109 In a second measurement campaign at JRC, the HEPaC, DiTEST, CAP3070 and DX280 counters were challenged  
110 with real diesel engine exhaust from a Euro 5b vehicle. Fig. 1b depicts the experimental setup at JRC. Soot from  
111 engine exhaust was passed through a water trap, a heated line (150 °C) to avoid water condensation, an ejector  
112 dilutor (DI-1000, Dekati, Finland), a catalytic stripper (Catalytic Instruments GmbH, Germany) to remove  
113 (semi)volatile organic matter, and was diluted to the required concentrations with a custom-made dilution bridge.  
114 It has been shown that the ejector dilutor does not affect the particle size distribution (Giechaskiel et al., 2009).  
115 PNC was recorded for several minutes, which allowed identifying long-time trends or drifts of the reported PNC.  
116 In addition, PNCs were averaged over a period of 1 min, thus the duration was similar to the duration of real PN-  
117 PTI tests which varies from 15 to 90 s. Mobility size distributions were measured by an SMPS, consisting of an  
118 <sup>85</sup>Kr source (3077A, TSI Inc., U.S.A.; purchased in 2021), a DMA 3081 and a CPC 3010 (TSI Inc., USA).

119 A Euro 5b vehicle with by-passed DPF was tested as real source of diesel soot. The vehicle generated size  
120 distributions with a GMD<sub>mob</sub> of 56.4 nm ± 0.7 nm. Diesel particles from the Euro 5b vehicle were collected on  
121 TEM grids and analysed as described above.

## 122 **3 Results**

### 123 **3.1 Aerosol properties**

124 [Particle number concentration measured by diffusion chargers depends on the average number of charges carried](#)  
125 [by each particle](#) (Fierz et al., 2011). Particle size and morphology have been shown to have an effect on the [number](#)  
126 [of charges carried by the particles and, thus, on the](#) counting efficiency of [diffusion charger based](#) PN-PTI  
127 instruments (see (Dhaniyala et al., 2011; Vasilatou et al., 2023) and references therein). [Soot particles form](#)  
128 [complex structures described by a fractal-like scaling law](#) (Mandelbrot, 1982), [and their mobility is influenced by](#)  
129 [their morphology \(described by the fractal dimension and fractal pre-factor\) and the momentum-transfer regime](#)  
130 (Filippov et al., 2000; Melas et al., 2014; Sorensen, 2011). [To characterise the soot particles produced by the](#)  
131 [different aerosol generators, the following aerosol properties were determined: particle size distribution, EC/TC](#)  
132 [ratio, primary particle size and fractal dimension. EC/TC ratio can also have an effect on the morphology of the](#)  
133 [soot particles. Soot particles formed in premixed flames \(i.e. high EC/TC\) exhibit a loose agglomerate structure](#)  
134 [where the primary particles are clearly distinguishable from one another, while soot generated in fuel-rich flames](#)  
135 [\(high OC/TC\) has a more compact structure and the primary particles tend to merge with each other \(see Fig. 3 in](#)  
136 (Ess et al., 2021b)).

137

138 The properties of the soot aerosols are summarised in Table 1. [Mobility size distributions are shown in Fig. S1.](#)139 **Table 1: Physical properties of the soot aerosols produced by the various combustion generators and the Euro 5b engine.**

Soot generator	Setpoint	$GMD_{mob}$ (nm)	GSD (nm)	EC/TC mass fraction (%)*	$d_{pp}$ (nm)**	$\rho_{eff}$ (g/cm <sup>3</sup> )***	$D_f^{\dagger\dagger}$
MISG	100 nm	103.3	1.76	86.2 ± 10	9.2 ± 2.8	0.91 ± 0.02	<a href="#">1.71 ± 0.03</a>
miniCAST 6204 C	50 nm	50.7	1.43	57.2 ± 8.9			
	70 nm	73.4	1.48	27.9 ± 4.6			
	80 nm	80.0	1.54	77.8 ± 9.0			
	100 nm	99.5	1.69	41.9 ± 6.5	21.6 ± 2.5	0.35 ± 0.04	<a href="#">1.54 ± 0.04</a>
miniCAST 5201 BC	50 nm	51.1	1.60	100 ± 18.5			
	70 nm fuel-lean	75.3	1.59	94.6 ± 15.6			
	70 nm fuel-rich	74.2	1.69	73.7 ± 11.4			
	80 nm	81.8	1.57	98.1 ± 15.3			
	100 nm fuel-lean	99.8	1.63	97.4 ± 9.6	15.8 ± 3.5 <sup>†</sup>	~ 0.4 <sup>†</sup>	<a href="#">1.58 ± 0.01</a>
	100 nm fuel-rich	101.9	1.58	65.7 ± 10.0	Primary particles are partly merged <sup>†</sup>	1.04 ± 0.16 <sup>†</sup>	<a href="#">1.71 ± 0.01</a>
bigCAST	50 nm	52.5	1.57	50.9 ± 11.7			
	70 nm	71.6	1.54	62.2 ± 13.3			
	80 nm	81.5	1.53	81.2 ± 8.8			
	100 nm	98.9	1.60	100.0 ± 9.0	24.5 ± 1.8	0.66 ± 0.04	<a href="#">1.66 ± 0.02</a>
Vehicle Euro 5b		56.4	2.12 ± 0.00	83.5 ± 20.5	19.7 ± 4.4		<a href="#">1.67 ± 0.03</a>

140 \* Uncertainties of the EC/TC mass fraction (downstream of the CS) are estimated to be in the range of 10-15 %.

141 Uncertainties due to the split point could not be quantified and were not taken into account.

142 \*\* Expanded uncertainty ( $k=2$ , 95 % confidence interval) determined as the twofold standard deviation of  $d_{pp}$ , of  
143 at least 20 primary particles of various mature soot particles divided by the square route of the number of  
144 measurements.145 \*\*\* Expanded uncertainty ( $k=2$ , 95 % confidence interval) determined as the twofold standard deviation of three  
146 measurements.

147 † Taken from (Ess et al., 2021b).

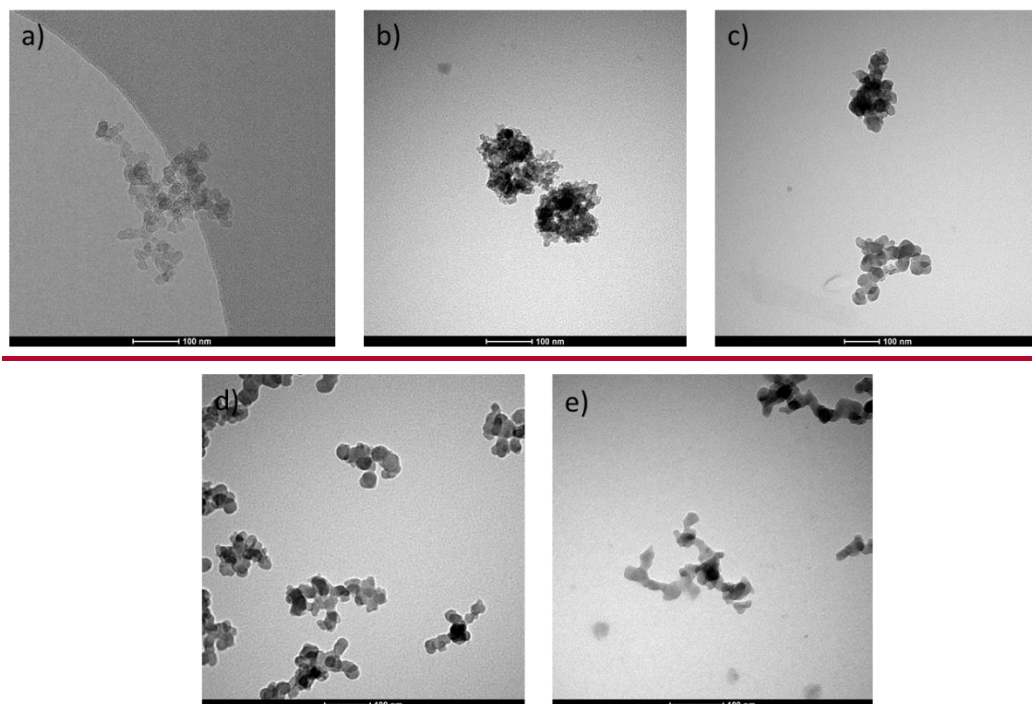
148 †† Expanded uncertainty ( $k=2$ , 95 % confidence interval) determined as the twofold standard deviation of at least  
149 [10 measurements.](#)

150

151 [The fractal dimension  \$D\_f\$  of soot particles with a nominal  \$GMD\_{mob}\$  of 100 nm was derived via image analysis of](#)  
152 [high-quality TEM-images using the FracLac feature of ImageJ 1.53e \(ImageJ, National institutes of Health, USA\).](#)

153 [In a first step, the greyscale TEM-images were converted into binary images utilizing the auto-convert function of](#)  
154 [FracLac. In a second step, the  \$D\_f\$  values were determined via the so-called box counting, averaging 12 rotations of](#)  
155 [each image. The  \$D\_f\$  values summarised in Table 1 represent the average values obtained from at least 10 particles](#)  
156 [for each type of soot. These values agree well with those reported in previous studies for bare \(i.e. freshly emitted\)](#)  
157 [soot particles \(Pang et al., 2022; Wang et al., 2017\).](#)

158 The effective density was determined for the 100 nm setpoints using an Aerodynamic Aerosol Classifier (AAC,  
159 Cambustion, UK) and a DMA (TSI Inc., USA) as described in (Tavakoli and Olfert, 2014). The lowest effective  
160 density ( $0.35 \pm 0.02 \text{ g/cm}^3$ ) was found for particles generated by the miniCAST 6204 C. Considering that these  
161 particles contain a high amount of OC, this value might seem at first glance to be low, but can be explained by the  
162 highly fractal-like structure of soot (Fig. 2e). In comparison, the miniCAST 5201 BC produced particles with an  
163 effective density of  $1.04 \pm 0.08 \text{ g/cm}^3$  when operated under fuel-rich conditions (i.e. high OC mass fraction), which  
164 is in line with the more compact structure as shown in (Ess et al., 2021b). Similarly, the MISG generated particles  
165 with an effective density of  $0.91 \pm 0.02 \text{ g/cm}^3$ . 100 nm particles generated by the bigCAST exhibited an  
166 intermediate effective density of  $0.66 \pm 0.02 \text{ g/cm}^3$ . [The results are in line with the calculated fractal dimension of](#)  
167 [soot particles, which increases from 1.54 for soot generated by the miniCAST 6204 C to 1.71 for soot generated](#)  
168 [by the MISG.](#)



169



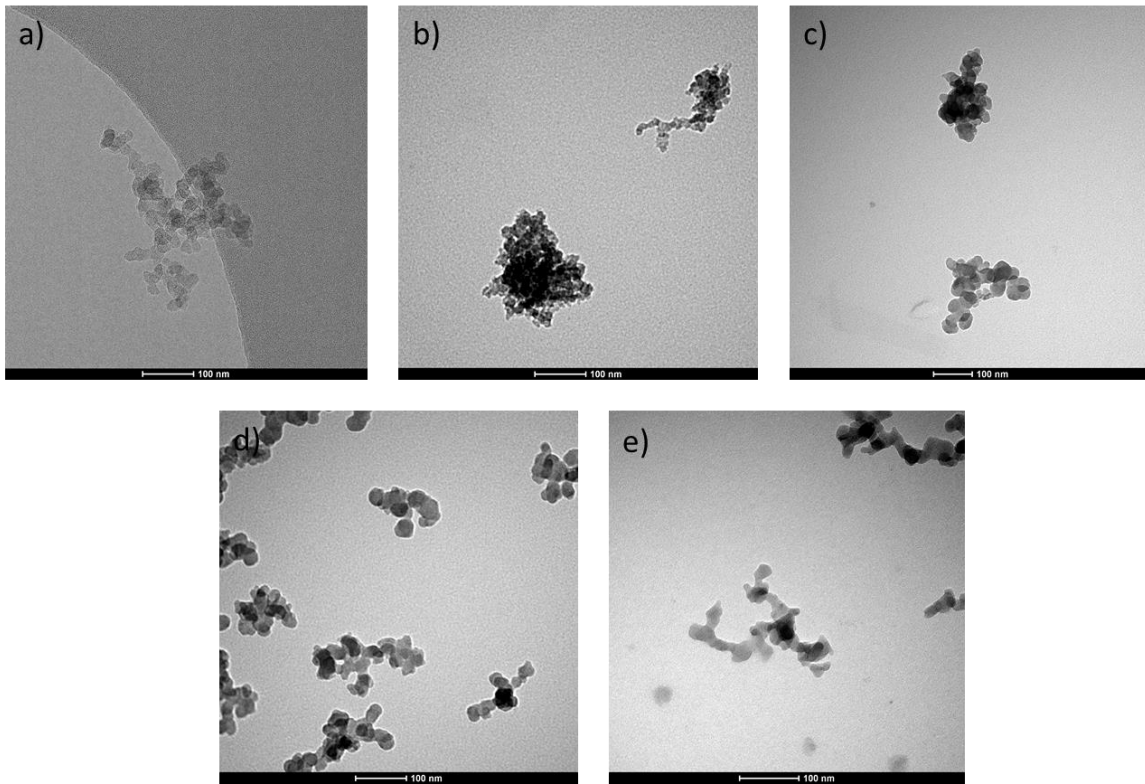


**Figure 2: TEM images of polydisperse soot particles generated by a) the miniCAST 5201 BC ( $GMD_{mob}$  of  $\sim 100$  nm, fuel-lean setpoint); b) the MISG ( $GMD_{mob}$  of  $\sim 100$  nm); c) by the Euro 5b test vehicle ( $GMD_{mob}$  of  $\sim 55$  nm); d) the prototype bigCAST ( $GMD_{mob}$  of  $\sim 100$  nm); and e) by the miniCAST 6204 C ( $GMD_{mob}$  of  $\sim 100$  nm). Further images are compiled in Figs. S2-S5 and in (Ess et al., 2021b).**

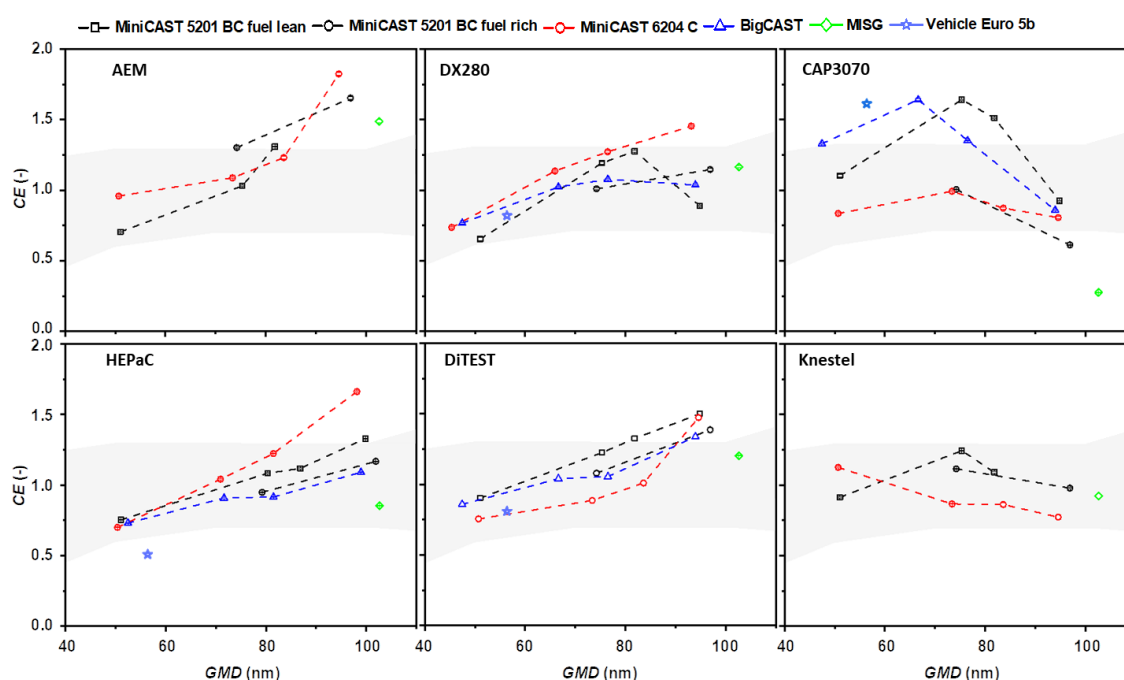
Soot particles generated by the bigCAST with a  $GMD_{mob}$  of  $\sim 100$  nm consist of primary particles with a diameter  $d_{pp} = 24.5 \text{ nm} \pm 1.8 \text{ nm}$ , whereas those from miniCAST 5201 BC (fuel lean setpoint) have an average primary particle size of  $12.3 \text{ nm} \pm 3.7 \text{ nm}$  at a similar  $GMD_{mob}$ . Soot generated by the MISG had a much smaller primary particle size ( $d_{pp}$  of  $9.2 \text{ nm} \pm 3.8 \text{ nm}$ ). The TEM images in Figs. 2b and S3 revealed [that some particles have a more compact soot structure than what reported by \(Kazemimanesh et al., 2019\) who used ethylene as fuel. This observation is in line with the relatively high particle effective density \( \$0.91 \text{ g/cm}^3\$ \) and fractal dimension \(1.71\) reported above.](#)

### 3.2 Counting efficiency (CE) profiles of PN-PTI counters

The CE profiles of the PN-PTI instruments under test were determined by dividing the reported number concentration by that measured with a reference condensation particle counter (NPET 3795, TSI Inc., USA). [The counting efficiency of the reference counter was taken into account during the data analysis.](#)

Figure 3 summarises the results obtained with the various laboratory-based combustion generators and the Euro 5b diesel vehicle. In general, the CE of PN-PTI instruments increased with increasing  $GMD_{mob}$ , in line with previous studies (Melas et al., 2023; Vasilatou et al., 2023). In the case of CAP3070, CE started to decrease at  $GMD_{mob} \geq 65$  nm, most probably due to built-in correction factors. [It cannot be ruled out that the measurement principle of the instrument, based on the so-called escaping current principle, plays also a role \(Lehtimäki, 1983\).](#) In general, for each PN-PTI instrument, the differences in CE when challenged with different soot aerosols of similar particle size were  $< 0.25$  at 50 nm and increased with size, but remained typically lower than 0.5. Higher differences were observed for CAP3070 at around 100 nm, probably related to the internal correction factors. This

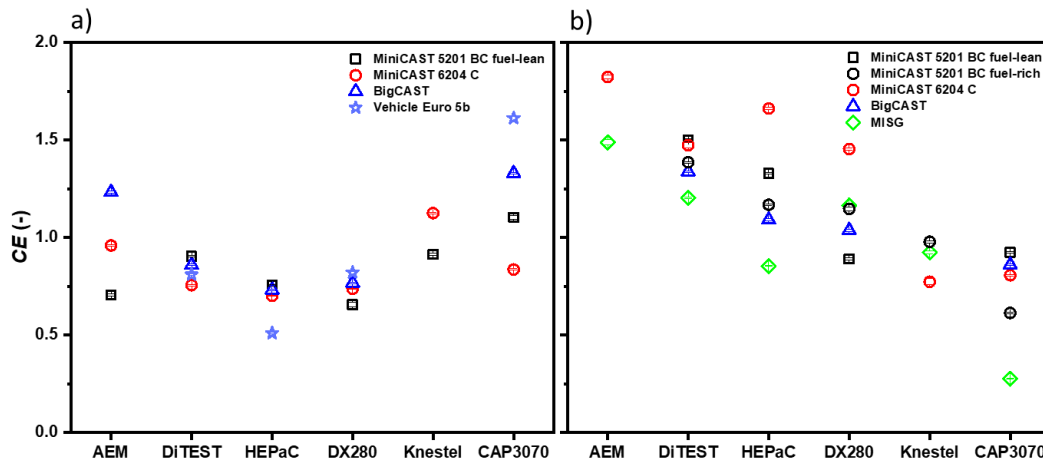
194 indicates that the exact morphology (e.g. primary particle size, effective density) of the test aerosol had an effect  
 195 on instrument performance [as expected from previous studies](#) (Dhaniyala et al., 2011). The response of each PN-  
 196 PTI model was, however, individual, making it difficult to draw any general trends. For instance, the CE of the  
 197 HEPaC was higher when measuring soot particles from the miniCAST 6204 C compared to soot of similar  
 198  $GMD_{mob}$  from the bigCAST. CAP3070 showed the opposite behaviour. At a  $GMD_{mob}$  of  $\sim 100$  nm, DX280  
 199 exhibited a higher CE with soot particles generated by the miniCAST 5201 BC under fuel-rich conditions (i.e.  
 200 lower EC/TC mass fraction) than at fuel-lean conditions (higher EC/TC mass fraction). CAP3070 showed again  
 201 the opposite behaviour. It is also worth mentioning that for the HePAC and DX280 instruments the measured CE  
 202 values scattered more at particle sizes larger than 90 nm. This supports the choice of soot with 50-90 nm mobility  
 203 diameter for the PN-PTI instruments verification linearity tests. [The counting efficiency of the different PN-PTI](#)  
 204 [counters as a function of time is shown in Figs. S6-S9 for a measurement duration of 2 min.](#)



205  
 206 **Figure 3: Influence of the type of soot generator/vehicle engine (bigCAST, miniCAST 5201 BC, miniCAST 6204 C,**  
 207 **MISG and Euro 5b diesel engine) on the counting efficiency (CE) of six different PN-PTI counters: AEM, HEPaC,**  
 208 **DiTEST, CAP3070, DX280, and Knestel. The grey-shaded area designates the upper and lower limits in the counting**  
 209 **efficiency as defined in the document "Commission Recommendation on particle number measurement for the periodic**  
 210 **technical inspection of vehicles equipped with compression ignition engines" (EU, 2023).**

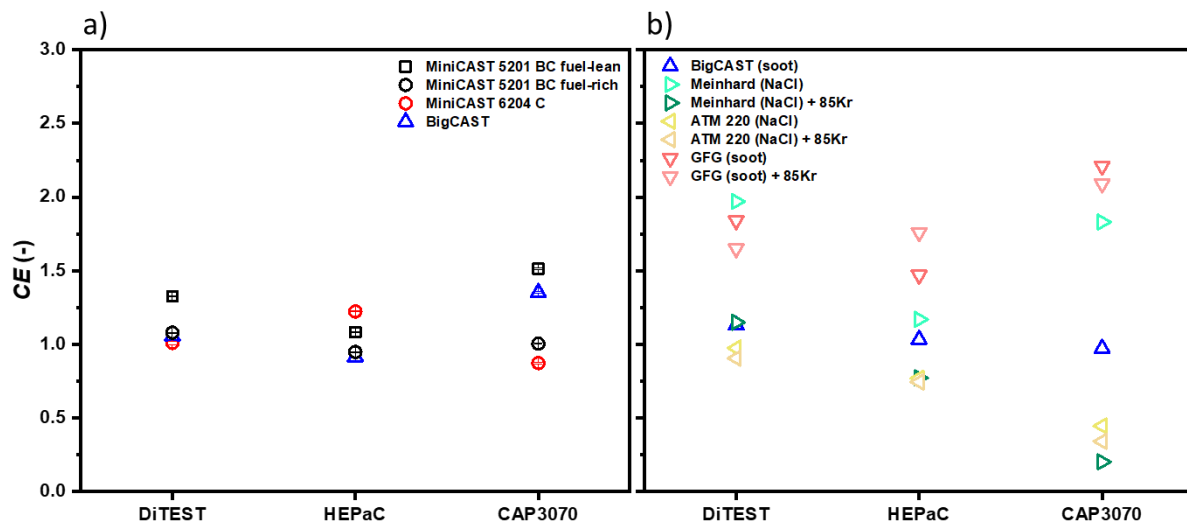
211 In the case of the DX280 and DiTEST, the CEs reported for the laboratory-generated soot ( $GMD_{mob}$  of about 50-  
 212 55 nm) showed an excellent agreement with the CE measured for diesel soot from a Euro 5b vehicle as shown in  
 213 Fig. 4a. In all other cases, deviations were observed. These remained typically within 0.25 units in CE but in one  
 214 case (for CAP3070) reached a factor of 2. Note that for real vehicle exhaust the tolerance (maximum permissible  
 215 error MPE) according to German regulations is  $\pm 50\%$  (PTB, 2021). In general, the data indicate that soot produced  
 216 by miniCAST and bigCAST generators simulate, in most cases, the properties of diesel soot by a Euro 5b vehicle  
 217 satisfactorily.





218  
 219 **Figure 4: Influence of the type of soot generator/engine (bigCAST, miniCAST 5201 BC, miniCAST 6204 C, MISG, Euro**  
 220 **5b vehicle) on the counting efficiencies (CE) of six different PN-PTI counters: AEM, HEPaC, DiTEST, CAP3070,**  
 221 **DX280, Knestel (the Knestel and AEM counters were not challenged with the Euro 5b vehicle since the Knestel counter**  
 222 **was sent for service and the performance of the AEM counter deteriorated during the measurement campaign at JRC).**  
 223 **The polydisperse test aerosols had a particle number concentration of  $\sim 100'000 \text{ cm}^{-3}$  and a  $\text{GMD}_{\text{mob}}$  of a) 50-55 nm and**  
 224 **b)  $\sim 100 \text{ nm}$ .**

225 As shown in Fig 4b, soot generated by the MISG ( $\text{GMD}_{\text{mob}} \sim 100 \text{ nm}$ ) led to CEs close to 1 for the DX280,  
 226 DiTEST, Knestel and HEPaC counters, and the CEs lied within the tolerance range defined in Germany and  
 227 Switzerland (the Netherlands and Belgium only specify a tolerance range for mobility diameters up to 80 nm). The  
 228 CE limit values were only exceeded in the case of the AEM and CAP3070 counters but this was most probably  
 229 due to a deterioration of the performance of the AEM instrument or an underestimated internal correction and an  
 230 overestimated internal correction factor in the case of CAP3070. Although the size of the soot generated by the  
 231 MISG ( $\text{GMD}_{\text{mob}} \geq 90 \text{ nm}$ ) tends to be larger than real soot from diesel engines (Kazemimanesh et al., 2019;  
 232 Moallemi et al., 2019; Senaratne et al., 2023), it's ease of operation combined with the affordable price make it an  
 233 attractive choice for PN-PTI verification in the laboratory.



234  
 235  
 236 **Figure 5: a) Influence of different soot aerosols with a  $\text{GMD}_{\text{mob}}$  of  $\sim 80 \text{ nm}$  on the counting efficiencies (CE) of three**  
 237 **different PN-PTI counters. b) Influence of different test aerosols (soot, NaCl and carbonaceous particles from a spark-**  
 238 **discharge generator) on the counting efficiencies (CE) of the same PN-PTI counters. The test aerosols had a  $\text{GMD}_{\text{mob}}$**   
 239 **of  $\sim 80 \text{ nm}$ . The data points are taken from (Vasilatou et al., 2023).**

240 The variation in the counting efficiency of the PN-PTI instruments when tested with soot particles from different  
241 combustion generators (Fig. 5a) is much smaller than that observed with test aerosols such as NaCl or particles  
242 from a spark-discharge generator with a similar  $GMD_{mob}$  (Fig. 5b) (Vasilatou et al., 2023). For instance,  
243 carbonaceous particles from a GFG spark-discharge generator (Palas GmbH, Germany) led to a CE of  $\geq 2$  in the  
244 case of CAP3070 and 1.7-1.8 in the case of DiTEST. On the contrary, CE remained typically in the range 0.7-1.3  
245 when soot was used as test aerosol, irrespective of the type of combustion generator (Fig. 5a). Further studies with  
246 more diesel test vehicles would be necessary to elucidate which type of laboratory-generated soot is the best proxy  
247 for diesel soot, keeping in mind that the properties of real diesel soot can also differ considerably, depending on  
248 the engine design, driving cycle and fuel properties (Hays et al., 2017; Wihersaari et al., 2020).

#### 249 **4 Recommendations**

250 Based on the results of this study, the following recommendations can be made:

- 251 1) Initial and follow-up verification of DC-based PN-PTI counters should ideally be performed with soot as test  
252 aerosol. If possible, the same type of combustion generator should be used for the determination of CE during  
253 type-examination and verification.
- 254 2) Low-cost soot generators can be a stable source of combustion particles and can be employed for PN-PTI  
255 verification using the appropriate setup correction factors. However, the GMD they produce should be in the  
256 range  $70 \pm 20$  nm in order to comply with the current linearity verification requirements in Europe.
- 257 3) Laboratory procedures for PN-PTI type-examination and verification should be further harmonised in Europe  
258 to avoid inconsistencies in the enforcement of PTI legislation. International round robin tests should be  
259 performed to examine whether a) the various PN-PTI instruments type-examined and verified in different  
260 European countries according to national regulations exhibit a similar performance and b) whether PN-PTI  
261 instruments verified in the same country but with different test aerosols identify defect DPFs in a consistent  
262 manner.

263 As highlighted in our previous study (Vasilatou et al., 2023), “setup correction factors” should be determined  
264 whenever verification is performed with particles other than soot to account for the effects of the test aerosol on  
265 the instrument's counting efficiency. These “setup correction factors” depend on both the aerosol physicochemical  
266 properties and the instrument's design, and need to be determined at the NMI level at regular intervals as drifts in  
267 the performance of the aerosol generator may occur. If “setup correction factors” are not applied or are inaccurate,  
268 the reliability of PTI will be compromised. The use of “setup correction factors” is more critical when nebulisers  
269 or spark-discharge generators are used, but special care should also be given to different flame soot generators.  
270 This calls for a closer collaboration between NMIs, state authorities, instrument manufacturers and verification  
271 centres to ensure fair implementation of regulations in Europe. Further harmonisation of the different PN-PTI  
272 type-examination procedures in Europe, e.g. in terms of the combustion generator, would be a valuable first step  
273 in order to determine meaningful correction factors for other test aerosols.

#### 274 **5 Conclusions**

275 The type of soot aerosol affected the response of six different DC-based PN-PTI counters tested in this study. Size  
276 and physicochemical properties of the test aerosol had effects on the CE of all counters. In most cases, the different

277 laboratory-generated soot aerosols resulted in deviations of 0.25 units in the counting efficiency of individual  
278 counters compared to Euro 5b diesel soot at similar mobility diameters (~50-60 nm). It is not entirely clear which  
279 type of laboratory-generated soot is the best proxy for real soot emitted by diesel vehicles as the response of the  
280 PN-PTI instruments to the different test aerosols was not uniform. It must also be kept in mind that the properties  
281 of diesel soot may vary depending on the engine specification and operation. Nevertheless, this study confirms  
282 that soot aerosols, irrespective of the generator model, are more suitable as test aerosols than NaCl, oil or particles  
283 from spark discharge generators. In view of these results, recommendations were made with regard to PN-PTI  
284 type-examination and verification.

#### 285 **Author contribution**

286 All authors designed the experiments. TH, DR and AM carried out the measurement campaigns. TH analysed the  
287 data with support from DR. KV prepared the manuscript with contributions from all co-authors.

#### 288 **Competing interests**

289 The authors declare no competing interests.

#### 290 **Acknowledgements**

291 TH, DR, and KV would like to thank Kevin Auderset and Christian Wälchli (both at METAS) for technical support  
292 and useful discussions. AM and BG would like to thank Dominique Lesueur and Andrea Bonamin for technical  
293 support.

#### 294 **Funding**

295 No external funding was used for this study.

#### 296 **References**

297 Anon: Regeling voertuigen 2019/328/NL, [online] Available from: [https://ec.europa.eu/growth/tools-](https://ec.europa.eu/growth/tools-databases/tris/en/search/?trisaction=search.detail&year=2019&num=328)  
298 [databases/tris/en/search/?trisaction=search.detail&year=2019&num=328](https://ec.europa.eu/growth/tools-databases/tris/en/search/?trisaction=search.detail&year=2019&num=328), 2019.

299 AU-Richtlinie: Richtlinie für die Durchführung der Untersuchung der Abgase von Kraftfahrzeugen nach Nummer  
300 4.8.2 der Anlage VIIIa StVZO und für die Durchführung von Abgasuntersuchungen an Kraftfahrzeugen nach §  
301 47a StVZO (AU-Richtlinie) (Stand 2021), [online] Available from: [https://beck-](https://beck-online.beck.de/Dokument?vpath=bibdata%5Cges%5Cbrd_013_2008_0196%5Ccont%5Cbrd_013_2008_0196.htm)  
302 [online.beck.de/Dokument?vpath=bibdata%5Cges%5Cbrd\\_013\\_2008\\_0196%5Ccont%5Cbrd\\_013\\_2008\\_0196.ht](https://beck-online.beck.de/Dokument?vpath=bibdata%5Cges%5Cbrd_013_2008_0196%5Ccont%5Cbrd_013_2008_0196.htm)  
303 [m](https://beck-online.beck.de/Dokument?vpath=bibdata%5Cges%5Cbrd_013_2008_0196%5Ccont%5Cbrd_013_2008_0196.htm), n.d.

304 Bischof, O. F., Weber, P., Bundke, U., Petzold, A. and Kiendler-Scharr, A.: Characterization of the Miniaturized  
305 Inverted Flame Burner as a Combustion Source to Generate a Nanoparticle Calibration Aerosol, *Emiss. Control*  
306 *Sci. Technol.*, 6(1), 37–46, doi:10.1007/S40825-019-00147-W/METRICS, 2020.

307 Botero, M. L., Londoño, J., Agudelo, A. F. and Agudelo, J. R.: Particle Number Emission for Periodic Technical  
308 Inspection in a Bus Rapid Transit System, *Emiss. Control Sci. Technol.*, 9, 128–139, doi:10.2139/ssrn.4246867,  
309 2023.

310 Burtscher, H., Lutz, T. and Mayer, A.: A New Periodic Technical Inspection for Particle Emissions of Vehicles,

311 Emiss. Control Sci. Technol. 2019 53, 5(3), 279–287, doi:10.1007/S40825-019-00128-Z, 2019.

312 Dhaniyala, S., Fierz, M., Keskinen, J. and Marjamäki, M.: Instruments Based on Electrical Detection of Aerosols

313 Aerosol Measurement, in *Aerosol Measurement: Principles, Techniques, and Applications*, edited by P. Kulkarni,

314 P. A. Baron, and K. Willeke, pp. 393–416, John Wiley & Sons, Inc., Hoboken, New Jersey., 2011.

315 Ess, M. N. and Vasilatou, K.: Characterization of a new miniCAST with diffusion flame and premixed flame

316 options: Generation of particles with high EC content in the size range 30 nm to 200 nm, *Aerosol Sci. Technol.*,

317 53(1), 29–44, doi:10.1080/02786826.2018.1536818, 2019.

318 Ess, M. N., Bertò, M., Keller, A., Gysel-Beer, M. and Vasilatou, K.: Coated soot particles with tunable , well-

319 controlled properties generated in the laboratory with a miniCAST BC and a micro smog chamber, *J. Aerosol Sci.*,

320 157, 105820, doi:10.1016/j.jaerosci.2021.105820, 2021a.

321 Ess, M. N., Bertò, M., Irwin, M., Modini, R. L., Gysel-Beer, M. and Vasilatou, K.: Optical and morphological

322 properties of soot particles generated by the miniCAST 5201 BC generator, *Aerosol Sci. Technol.*, 55(7), 828–

323 847, doi:10.1080/02786826.2021.1901847, 2021b.

324 EU: COMMISSION RECOMMENDATION (EU) 2023/688 of 20 March 2023 on particle number measurement

325 for the periodic technical inspection of vehicles equipped with compression ignition engines, *Off. J. Eur. Union*,

326 (715), 46–64 [online] Available from: [https://eur-lex.europa.eu/legal-](https://eur-lex.europa.eu/legal-content/EN/TXT/?uri=CELEX%3A32023H0688)

327 [content/EN/TXT/?uri=CELEX%3A32023H0688](https://eur-lex.europa.eu/legal-content/EN/TXT/?uri=CELEX%3A32023H0688), 2023.

328 Fierz, M., Houle, C., Steigmeier, P. and Burtscher, H.: Design, calibration, and field performance of a miniature

329 diffusion size classifier, *Aerosol Sci. Technol.*, 45(1), 1–10, doi:10.1080/02786826.2010.516283, 2011.

330 Filippov, A. V., Zurita, M. and Rosner, D. E.: Fractal-like aggregates: Relation between morphology and physical

331 properties, *J. Colloid Interface Sci.*, 229(1), 261–273, doi:10.1006/jcis.2000.7027, 2000.

332 Frank, Adam, Olfert, J., Wong, K.-F., Kunert, S. and Richter, J. M.: Effect of Engine-Out Soot Emissions and the

333 Frequency of Regeneration on Gasoline Particulate Filter Efficiency, *SAE Tech. Pap.*, 2020-01-14,

334 doi:10.4271/2020-01-1431, 2020.

335 Giechaskiel, B. and Melas, A.: Comparison of Particle Sizers and Counters with Soot-like, Salt, and Silver

336 Particles, *Atmosphere (Basel)*, 13(10), doi:10.3390/atmos13101675, 2022.

337 Giechaskiel, B., Ntziachristos, L. and Samaras, Z.: Effect of ejector dilutors on measurements of automotive

338 exhaust gas aerosol size distributions, *Meas. Sci.*, 20, 045703, doi:10.1088/0957-0233/20/4/045703, 2009.

339 Giechaskiel, B., Forloni, F., Carriero, M., Baldini, G., Castellano, P., Vermeulen, R., Kontses, D., Fragkiadoulakis,

340 P., Samaras, Z. and Fontaras, G.: Effect of Tampering on On-Road and Off-Road Diesel Vehicle Emissions,

341 *Sustainability*, 14(10), 6065, doi:10.3390/su14106065, 2022.

342 Hays, M. D., Preston, W., George, B. J., George, I. J., Snow, R., Faircloth, J., Long, T., Baldauf, R. W. and

343 McDonald, J.: Temperature and Driving Cycle Significantly Affect Carbonaceous Gas and Particle Matter

344 Emissions from Diesel Trucks, *Energy and Fuels*, 31(10), 11034–11042, doi:10.1021/acs.energyfuels.7b01446,

345 2017.

346 Kazemimanes, M., Moallemi, A., Thomson, K., Smallwood, G., Lobo, P. and Olfert, J. S.: A novel miniature

347 inverted-flame burner for the generation of soot nanoparticles, *Aerosol Sci. Technol.*, 53(2), 184–195,

348 doi:10.1080/02786826.2018.1556774, 2019.

349 Kesselmeier, J. and Staudt, M.: An Overview on Emission, Physiology and Ecology, *J. Atmos. Chem.*, 33, 23–88

350 [online] Available from: [https://link-springer-](https://link.springer-com.ez27.periodicos.capes.gov.br/content/pdf/10.1023%2FA%3A1006127516791.pdf)

351 [com.ez27.periodicos.capes.gov.br/content/pdf/10.1023%2FA%3A1006127516791.pdf](https://link.springer-com.ez27.periodicos.capes.gov.br/content/pdf/10.1023%2FA%3A1006127516791.pdf), 1999.

352 Kheirbek, I., Haney, J., Douglas, S., Ito, K. and Matte, T.: The contribution of motor vehicle emissions to ambient  
353 fine particulate matter public health impacts in New York City: A health burden assessment, *Environ. Heal. A*  
354 *Glob. Access Sci. Source*, 15(1), doi:10.1186/s12940-016-0172-6, 2016.

355 Kurniawan, A. and Schmidt-Ott, A.: Monitoring the soot emissions of passing cars, *Environ. Sci. Technol.*, 40(6),  
356 1911–1915, doi:10.1021/es051140h, 2006.

357 Lehtimäki, M.: Modified Electrical Aerosol Detector, in *Aerosols in the Mining and Industrial Work*  
358 *Environments: Instrumentation (Vol. 3)*, edited by B. Y. H. Liu and V. A. Marple, pp. 1135–1143, Ann Arbor  
359 Science Publishers., 1983.

360 Ligterink, N. E.: *Diesel Particle Filters.*, 2018.

361 Mandelbrot, B. B.: *The fractal geometry of nature*, Freeman, W. H., San Francisco., 1982.

362 Melas, A., Selleri, T., Suarez-Bertoa, R. and Giechaskiel, B.: Evaluation of solid particle number sensors for  
363 periodic technical inspection of passenger cars, *Sensors*, 21(24), 8325, doi:10.3390/s21248325, 2021.

364 Melas, A., Selleri, T., Suarez-Bertoa, R. and Giechaskiel, B.: Evaluation of Measurement Procedures for Solid  
365 Particle Number (SPN) Measurements during the Periodic Technical Inspection (PTI) of Vehicles, *Int. J. Environ.*  
366 *Res. Public Health*, 19(13), 7602, doi:10.3390/ijerph19137602, 2022.

367 Melas, A., Vasilatou, K., Suarez-Bertoa, R. and Giechaskiel, B.: Laboratory measurements with solid particle  
368 number instruments designed for periodic technical inspection (PTI) of vehicles, *Measurement*, 215(April),  
369 112839, doi:10.1016/j.measurement.2023.112839, 2023.

370 Melas, A. D., Isella, L., Konstandopoulos, A. G. and Drossinos, Y.: Friction coefficient and mobility radius of  
371 fractal-like aggregates in the transition regime, *Aerosol Sci. Technol.*, 48(12), 1320–1331,  
372 doi:10.1080/02786826.2014.985781, 2014.

373 Moallemi, A., Kazemimanesh, M., Corbin, J. C., Thomson, K., Smallwood, G., Olfert, J. S. and Lobo, P.:  
374 Characterization of black carbon particles generated by a propane-fueled miniature inverted soot generator, *J.*  
375 *Aerosol Sci.*, 135, 46–57, doi:10.1016/J.JAEROSCI.2019.05.004, 2019.

376 Pang, Y., Wang, Y., Wang, Z., Zhang, Y., Liu, L., Kong, S., Liu, F., Shi, Z. and Li, W.: Quantifying the Fractal  
377 Dimension and Morphology of Individual Atmospheric Soot Aggregates, *J. Geophys. Res. Atmos.*, 127(5),  
378 e2021JD036055, doi:10.1029/2021JD036055, 2022.

379 PTB: PTB-Anforderungen 12.16 „Partikelzähler“ (05/2021)., [online] Available from:  
380 <https://doi.org/10.7795/510.20210623>, 2021.

381 Senaratne, A., Olfert, J., Smallwood, G., Liu, F., Lobo, P. and Corbin, J. C.: Size and light absorption of miniature-  
382 inverted-soot-generator particles during operation with various fuel mixtures, *J. Aerosol Sci.*, 170(February),  
383 106144, doi:10.1016/j.jaerosci.2023.106144, 2023.

384 Sorensen, C. M.: The mobility of fractal aggregates: A review, *Aerosol Sci. Technol.*, 45(7), 765–779,  
385 doi:10.1080/02786826.2011.560909, 2011.

386 Tavakoli, F. and Olfert, J. S.: Determination of particle mass, effective density, mass-mobility exponent, and  
387 dynamic shape factor using an aerodynamic aerosol classifier and a differential mobility analyzer in tandem, *J.*  
388 *Aerosol Sci.*, 75, 35–42, doi:10.1016/j.jaerosci.2014.04.010, 2014.

389 US-EPA: *Integrated Science Assessment for Particulate Matter.* [online] Available from:  
390 <https://www.epa.gov/isa/integrated-science-assessment-isa-particulate-matter>, 2019.

391 UVEK: *Verordnung des UVEK über Wartung und Nachkontrolle von Motorwagen betreffend Abgas- und*  
392 *Rauchemissionen (SR 741.437),* , 1–18 [online] Available from: <https://www.fedlex.admin.ch/eli/cc/2002/596/de>,



393 2023.

394 VAMV: Verordnung des EJPD über Abgasmessmittel für Verbrennungsmotoren (VAMV), [online] Available  
395 from: <https://www.fedlex.admin.ch/eli/cc/2006/251/de>, 2018.

396 Vasilatou, K., Kok, P., Pratzler, S., Nowak, A., Waheed, A., Buekenhoudt, P., Auderset, K. and Andres, H.: New  
397 periodic technical inspection of diesel engines based on particle number concentration measurements, OIML Bull.,  
398 LXIII, 11–16 [online] Available from:  
399 [https://www.oiml.org/en/publications/bulletin/pdf/oiml\\_bulletin\\_july\\_2022.pdf](https://www.oiml.org/en/publications/bulletin/pdf/oiml_bulletin_july_2022.pdf), 2022.

400 Vasilatou, K., Wälchli, C., Auderset, K., Burtscher, H., Hammer, T., Giechaskiel, B. and Melas, A.: Effects of the  
401 test aerosol on the performance of periodic technical inspection particle counters, *J. Aerosol Sci.*, 172(January),  
402 doi:10.1016/j.jaerosci.2023.106182, 2023.

403 Wang, Y., Liu, F., He, C., Bi, L., Cheng, T., Wang, Z., Zhang, H., Zhang, X., Shi, Z. and Li, W.: Fractal  
404 Dimensions and Mixing Structures of Soot Particles during Atmospheric Processing, *Environ. Sci. Technol. Lett.*,  
405 4(September 2019), 487–493, doi:10.1021/acs.estlett.7b00418, 2017.

406 WHO: WHO global air quality guidelines, *Coast. Estuar. Process.*, 1–360 [online] Available from:  
407 <https://apps.who.int/iris/handle/10665/345329>, 2021.

408 Wihersaari, H., Pirjola, L., Karjalainen, P., Saukko, E., Kuuluvainen, H., Kulmala, K., Keskinen, J. and Rönkkö,  
409 T.: Particulate emissions of a modern diesel passenger car under laboratory and real-world transient driving  
410 conditions, *Environ. Pollut.*, 265, doi:10.1016/j.envpol.2020.114948, 2020.

411

412

